

1
2
3
4
5
6
7
8
9
10
11
12
13
14
15
16
17
18
19
20
21
22
23
24

Am J Physiol Endo Metab: Innovative Methodology (E-00182-2016R1)

Quantifying rates of glucose production in vivo following an intraperitoneal tracer bolus.

Sheng-Ping Wang*, Dan Zhou*, Zuliang Yao*, Santhosh Satapati*, Ying Chen, Natalie A. Daurio, Aleksandr Petrov, Xiaolan Shen, Daniel Metzger, Wu Yin, Andrea Nawrocki, George J Eiermann, Joyce Hwa, Craig Fancourt, Corin Miller, Kithsiri Herath, Thomas P. Roddy, Deborah Slipetz, Mark D. Erion, Stephen F. Previs# and David E. Kelley

Merck Research Laboratories, 2000 Galloping Hill Road, Kenilworth, NJ 07033

#Corresponding author: Stephen F. Previs, Ph.D., Merck & Co., 2000 Galloping Hill Road, Kenilworth, NJ 07033, Tel: 732-594-3364; E-mail: stephen_previs@merck.com

*Each made equally critical contributions to the development of the work discussed here.

Running title: Coupling stable isotope tracers and mass spectrometry-based analyses.

Keywords: type 2 diabetes, insulin resistance, stable isotopes, tracer kinetics, animal models,

Acknowledgments: We thank Xiaoli Ping, Xuening Hong, Aimee Burton, Loise Gichuru, Chris Nunes and Irene Capodanno for their time and expertise in performing the rodent surgeries.

25 **Abstract**

26 Aberrant regulation of glucose production makes a critical contribution to the impaired glycemic control
27 that is observed in Type 2 diabetes. Although isotopic tracer methods have proven to be informative in
28 quantifying the magnitude of such alterations, it is presumed that one must rely on venous access to
29 administer glucose tracers which therein presents obstacles for the routine application of tracer
30 methods in rodent models. Since intraperitoneal injections are readily used to deliver glucose challenges
31 and/or dose potential therapeutics, we hypothesized that this route could also be used to administer a
32 glucose tracer. The ability to then reliably estimate glucose flux would require attention towards setting
33 a schedule for collecting samples and choosing a distribution volume. For example, glucose production
34 can be calculated by multiplying the fractional turnover rate by the pool size. We have taken a step-wise
35 approach to examine the potential of using an intraperitoneal tracer administration in rat and mouse
36 models. First, we compared the kinetics of [U-¹³C]glucose following either an intravenous or an
37 intraperitoneal injection. Second, we tested whether the intraperitoneal method could detect a
38 pharmacological manipulation of glucose production. Finally, we contrasted a potential application of
39 the intraperitoneal method against the glucose-insulin clamp. We conclude that it is possible to (i)
40 quantify glucose production using an intraperitoneal injection of tracer and (ii) derive a “glucose
41 production index” by coupling estimates of basal glucose production with measurements of fasting
42 insulin concentration; this yields a proxy for clamp-derived assessments of insulin sensitivity of
43 endogenous production.

44

45

46 **Introduction**

47 Type 2 diabetes is typically characterized by the presence of fasting hyperglycemia, which largely results
48 from a disruption in the control of basal glucose production (9; 10). Numerous investigators have aimed
49 to quantify glucose production using isotopic tracers in order to better understand the pathophysiology
50 surrounding Type 2 diabetes and states of insulin resistance (27; 28; 38). In that regard, emphasis has
51 been placed on coupling tracer kinetics with the use of a “glucose-insulin clamp” in order to address
52 questions regarding the insulin sensitivity of endogenous glucose production (10; 16; 38). Given the
53 increase in obesity and the prevalence of insulin resistance it comes as no surprise that many methods
54 have been adapted for use in rodent models where one can readily manipulate gene expression and/or
55 examine the efficacy and mechanism of action of novel therapeutics (1-3; 21). Unfortunately, studies are
56 typically low throughput since animals require catheterization. Herein we have considered an
57 alternative modality for quantifying glucose production in vivo. Namely, we suspected that one could
58 quantify glucose flux using an intraperitoneal bolus of a tracer which would then allow investigators to
59 envision higher throughput studies in rodent models while helping to conserve resources. The rationale
60 for considering this approach is outlined below.

61
62 Rates of glucose production can be quantified by administering an isotopically labeled tracer and then
63 measuring its dilution (28; 41). If one restricts questions surrounding glucose production to conditions of
64 a metabolic steady-state, e.g. determine rates of glucose production in a post-absorptive period, then
65 investigators must contend with two central issues when planning a study. For example, one must
66 consider (i) what type of tracer should be given and (ii) how should it be administered?

67
68 Classic studies relied on the use of radiolabeled tracers and generated interesting data regarding how
69 the type of tracer (i.e. ^3H vs ^{14}C) and the positional labeling could affect one’s interpretation of the
70 metabolic rate(s) (18-20). For example, it was recognized that specific glucose tracers would experience
71 different dilutions and that this could be explained via glucose cycling (18-20; 41). The adaptation of
72 stable isotope tracers confirmed the early observations and allowed investigators to simultaneously mix
73 multiple isotopes in order to quantify the magnitude of the different flux rates (31). Since mass
74 spectrometry and NMR can separate the different species, it is possible to envision the routine
75 implementation of such methods (13).

76
77 As our understanding of physiology has advanced, in part due to the application of mathematical
78 models, it became clear that one could use different approaches for administering a tracer. For example,
79 one could dose a tracer via a single intravenous injection, a continuous infusion or a primed-infusion
80 (27; 28; 41). Glucose flux rates are then determined by measuring the dilution of the isotope and
81 estimating the pool size (e.g. when using the intravenous bolus approach) or by simply measuring the
82 rate of tracer dilution (e.g. when using either a constant infusion and/or a primed-infusion) (28; 38).
83 Note that this logic assumes a single (well-mixed) compartment model, which appears to be reasonably
84 valid in rodent models and in basal conditions in humans (4; 5; 14; 30).

85

86 Given the extensive history in this field, investigators have several choices regarding the design of
87 preclinical studies. However, it is unfortunate that none of the described protocols are well suited for
88 rapid (user friendly) phenotyping of rodent models. Namely, the presumption is that investigators must
89 rely on a surgical manipulation to implant catheters and/or utilize protocols which require a certain
90 degree of care in order to make delicate tail vein injections. We hypothesized that one could quantify
91 rates of glucose flux by administering a glucose tracer via an intraperitoneal bolus. This approach would
92 be analogous to the use of an intravenous (e.g. tail vein) injection of a tracer but could, in principle, be
93 easier to implement by less specialized associates and/or facilitate larger scale studies. Indeed, the use
94 of intraperitoneal administration is not necessarily new (42), one can expect a reasonably rapid
95 distribution of substances into the circulation (40). Herein we discuss the development and use of an
96 intraperitoneal bolus method for quantifying glucose flux in rodents.

97

98 **Materials and Methods**

99 *Biological.* A pilot study was conducted in 5 week old female ZDF (fZDF) rats that had been maintained
100 on a high fat diet (D10111701, Research Diets, New Brunswick, NJ; 48% kcal from fat, 18% kcal from
101 protein and 34% kcal from carbohydrates, 4.8 kcal / g food); tracer studies were performed following a 3
102 week feeding period. Food was removed at 8AM on the day of the study, 5 hours later rats were dosed
103 with [U-¹³C]glucose (0.04 g per kg) using either a tail vein injection or intraperitoneal bolus (the dosing
104 volume was ~ 5 ml per kg). The concentration of circulating glucose was immediately determined using a
105 glucometer, a small sample of whole blood (~ 5 ul) was collected into 5 ul 0.1N citrate buffer at various
106 time points and used to determine the isotopic labeling. The isotopic enrichment of circulating glucose
107 was determined as follows: during the intravenous bolus protocol samples were collected at 0, 5, 15, 30,
108 45, 60, 75, 90, 120 and 150 minutes and during the intraperitoneal bolus protocol samples were
109 collected at 0, 15, 30, 45, 60, 75, 90, 120 and 150 minutes post tracer administration.

110

111 A second study was conducted in fZDF rats following treatment with Rosiglitazone. This study relied on
112 the same diet and conditions as noted above, Rosiglitazone or 0.5% methylcellulose (vehicle) was
113 administered using an oral gavage (10 mg drug per kg body weight per day, the total dosing ran for 5
114 days over the last week of the high fat feeding period). The glucose tracer protocol and sampling
115 scheme followed the same outline as above for the intraperitoneal method.

116

117 Studies were run to quantify glucose production in mouse models using the following protocols. Male
118 C57Bl/6J mice started on a high fat diet at 6 weeks of age (D12492, Research Diets, New Brunswick, NJ;
119 60% kcal from fat, 20% kcal from protein and 20% kcal from carbohydrates, 5.2 kcal / g food), they were
120 maintained on this diet for 16 weeks. To estimate glucose production, food was removed at 8AM and
121 mice were dosed at 1PM with [U-¹³C]glucose (0.05 g per kg) using the tail vein injection or
122 intraperitoneal bolus (the dosing volume was ~ 5 ml per kg), i.e. a similar protocol to that used in rats.
123 Whole blood (~ 5 ul) was collected into 5 ul 0.1N citrate buffer at 5, 15, 30, 45, 60, 75, 90 and 120
124 minutes post-injection, the 5 minutes sample was not collected for the intraperitoneal protocol.

125

126 A second study was conducted in ob/ob mice following treatment with Pioglitazone. In all cases we
127 studied 10 week old male animals. The ob/ob mice were randomized and either dosed with 0.5%
128 methylcellulose (vehicle) or 10 mg per kg of Pioglitazone (orally, QD at ~ 8-9AM) for 5 days, control mice
129 (ob/+) were dosed with 0.5% methylcellulose (vehicle) for the same period. To estimate glucose
130 production, food was removed at 8AM and mice were dosed at 1PM with [U-¹³C]glucose (0.05 g per kg)
131 using an intraperitoneal bolus (the dosing volume was ~ 5 ml per kg), i.e. a similar protocol to that used
132 in studies noted earlier. Whole blood (~ 5 ul) was collected into 5 ul 0.1N citrate buffer at 0, 30, 60, 90
133 and 120 minutes post-tracer.

134
135 Glucose-insulin clamps were performed using the following protocol. Rodents (5 week old fZDF rats)
136 were purchased from Charles River and fed a high-fat diet (Research Diets, D10111701) for 3 weeks to
137 induce hyperinsulinemia and hyperglycemia. Seven days prior to the clamps, rats were anesthetized and
138 dual indwelling catheters (carotid artery and jugular vein) were surgically implanted. Starting 2 days
139 after the surgery, rats were dosed with either 0.5% methylcellulose (vehicle) or Rosiglitazone (5 mg per
140 kg, orally, QD at ~ 8-9 AM) for 5 days. After 5 days of treatment, rats were fasted for ~ 6 hours and
141 hyperinsulinemic-euglycemic clamps were performed as described previously (39). Briefly ~ 4 hours into
142 the fast, a baseline blood sample was drawn (t = -90 min) and a 100 µg per minute bolus infusion of [U-
143 ¹³C₆]glucose was given for 10 minutes, this was followed by a continuous infusion for 80 minutes (at 25
144 µg per minute) to achieve a steady-state. Two blood draws (t = -10 and 0 minutes) were made to
145 measure basal glucose turnover. After the blood collection at t = 0 minutes, insulin (Humulin, 25 mU per
146 min per kg) was infused and blood glucose was maintained at ~ 120 to 140 mg per dl by variable infusion
147 of 25% dextrose solution (this solution was enriched to ~ 2.5% with [U-¹³C₆]glucose). Blood samples
148 were collected at various time points (t = 90, 100, 110 and 120 minutes) during the steady-state phase
149 of the clamp and stored until further analysis.

150
151 Mice (5 week old male ob/ob mice) were purchased from Jackson Laboratories and allowed to acclimate
152 for one week, they were then fed regular chow or chow mixed with Pioglitazone (300 mg per kg diet).
153 After 3 weeks on the respective diets, mice were surgically implanted with dual indwelling catheters
154 (carotid artery and jugular vein) and allowed to recover. On day 7 following the surgery, mice were
155 fasted for ~ 6 hours and hyperinsulinemic-euglycemic clamps were performed as described above.

156
157 A final group of rats was studied to determine if we could quantify differences in short- vs long-term
158 fasting. In this case, Sprague-Dawley rats were maintained on normal carbohydrate-based chow. Food
159 was removed for 4 hours before an intraperitoneal bolus of [U-¹³C₆]glucose was given (0.015 g per kg),
160 blood was sampled at various times over the next 150 minutes. Rats were allowed to recover and then
161 maintained again for 1 week in their standard cages with free access to their carbohydrate-based chow,
162 the tracer study was then repeated however following an 18 hour fast. [U-¹³C₆]Glucose was again given
163 via an intraperitoneal bolus and samples were collected over the same period as in the study with short-
164 term fasting.

165

166 *Analytical.* The enrichment of glucose was determined as follows. Samples were vigorously mixed after
 167 the addition of 100 ul methanol, following a brief centrifugation the supernatant was removed and
 168 evaporated to dryness under a stream of nitrogen. The residue was reacted with 50 ul of hydroxylamine
 169 hydrochloride (25 mg per ml of pyridine) at 65°C for 30 min, 50 ul acetic anhydride was then added and
 170 the heating was continued for another 30 min. Samples were then evaporated to dryness under a
 171 stream of nitrogen and the residue was dissolved in 70 ul ethyl acetate prior to GCMS analyses. Samples
 172 were analyzed in an Agilent 5973 mass spectrometer coupled with a 6890N GC (HP 5 column, 175°C
 173 initial temperature, hold for 0 min and ramp to 300°C at 35°C per min, hold for 1 min). Data were
 174 acquired using selected ion monitoring under electron impact ionization (m/z 314 to 319, 10 ms dwell
 175 per ion).

176
 177 Note that although M+6 glucose is administered this analytical method actually measures the
 178 enrichment using the M+5 isotopomer. We have determined that there is negligible recycling of ¹³C
 179 during this period which therein avoids any potential interference. For example, the enrichment in M+1,
 180 2 or 3 isotopomers is less than 2% at its maximum (this was determined using the same derivative but
 181 running the analyses using chemical ionization in order to quantify the full isotope spectrum,
 182 unpublished observations). We specifically chose this derivatization and analytical scheme since the
 183 chemical workup is straightforward and robust and the analytics can be performed with a somewhat
 184 basic mass spectrometer operated in a simple mode.

185
 186 Insulin concentrations were determined using a standard kit (AlphaLISA Insulin, PerkinElmer).

187
 188 *Calculations.* The fractional turnover rate of glucose was estimated by measuring the decrease in
 189 glucose enrichment, data were fit using a linear regression analyses (i.e. the y-axis labeling was
 190 converted to a natural log scale and the slope was determined using GraphPad Prism). The glucose pool
 191 size was estimated by measuring the concentration of glucose and then assuming a volume of
 192 distribution that was equivalent to 20% of body weight. In cases when [U-¹³C]glucose was administered
 193 using an intravenous bolus the glucose pool size was determined from the initial enrichment, typically
 194 using samples that were collected 5 minutes after the tracer was administered, i.e. pool size (mg) = dose
 195 of tracer (mg) / initial labeling (30; 41). Absolute rates of glucose production were determined by
 196 multiplying the fractional turnover by the pool size (30; 41).

197
 198 In cases where glucose-insulin clamps were used to study glycemic control, glucose flux was determined
 199 using steady-state analyses. Namely, basal rates of appearance (Ra) of glucose are equal to rates of
 200 endogenous glucose production (EGP) and determined using the standard equation:

$$Ra (mg \times kg^{-1} \times min^{-1}) = \text{tracer infusion} (mg \times kg^{-1} \times min^{-1}) \times [(IE_{infusate} / IE_{plasma}) - 1]$$

201
 202 where IE represents isotopic enrichment. During the hyperinsulinemic clamp period the tracer infusion
 203 again yields the Ra however EGP is determined after subtracting the glucose infusion rate using the
 204 equation:

$$EGP = Ra - \text{glucose infusion rate}$$

205
 206 where all flux rates are expressed as mg x kg⁻¹ x min⁻¹.

207

208 **Results**

209 Figure 1 demonstrates the temporal profile of glucose concentration and isotopic enrichment in high-fat
210 fed fZDF rats and high-fat fed C57Bl/6J mice following either an intravenous or intraperitoneal bolus of
211 [U-¹³C]glucose. As shown, the glucose concentration remained constant regardless of the modality that
212 was used to administer the tracer dose of [U-¹³C]glucose in rats (Panel A) but there was transient
213 increase in glucose concentration following the intravenous tracer administration in mice (Panel C).
214 Regardless of the model, and as expected, there is a more rapid rise in plasma enrichment following the
215 intravenous tracer bolus; the slower rise following the intraperitoneal tracer injection is consistent with
216 the hypothesis of delayed tracer entry into the central compartment (Panel B and D).

217

218 Table 1 contains the critical parameters that are derived from the primary concentration and
219 enrichment data (contained in Figure 1) and demonstrates the apparent rates of endogenous glucose
220 production. In the rat model, glucose turnover was determined using data that were collected from 45
221 to 120 minutes post-tracer administration. These time points were chosen based on the data obtained
222 in animals that had received an intraperitoneal bolus. Clearly, the delayed entry of tracer following the
223 intraperitoneal bolus requires that the sampling be shifted to a region where one can observe a steadily
224 decreasing enrichment, i.e. time points that are sampled after the tracer has moved from the
225 intraperitoneal space and into the central compartment. The data in the rat model are relatively
226 consistent regardless of the modality that is used for administering the tracer. Note that we observed
227 comparable fractional rates of turnover and equivalent estimates of pool size, therefore we calculated
228 nearly identical rates of endogenous glucose production in fZDF rats (Table 1).

229

230 Regardless of the modality that was used to administer the tracer the mouse model also showed
231 comparable fractional rates of glucose turnover, however, there are clear differences between the
232 apparent pool size. For example, if we used the initial dilution method, i.e. pool size (mg) = tracer dose
233 (mg) / initial labeling, we would conclude that the glucose pool is 43 ± 4 mg (mean \pm sem). This value
234 overestimates the pool size that is inferred by measuring the baseline concentration and assuming a
235 distribution volume that is $\sim 20\%$ of body weight (i.e. ~ 24 mg as shown in Table 1). The difference is \sim
236 1.8-fold (i.e. ~ 43 vs ~ 24 mg) and is consistent with the acute change in glucose concentration that is
237 seen 5 minutes after the intravenous bolus is administered, i.e. the glucose concentration increased \sim
238 1.6-fold (from ~ 195 to ~ 315 mg per dl). The stress that is associated with the intravenous tracer
239 injection and the effect this had on estimating the initial tracer dilution suggested to us that it is best to
240 estimate the pool size by assuming a distribution volume that is $\sim 20\%$ of body weight. As shown in
241 Table 1, we observed reasonably good agreement between the apparent rates of endogenous glucose
242 production regardless of how the tracer was administered. Obviously, we obtained a slightly higher
243 value in mice receiving an intravenous bolus, which is not surprising given the transient perturbation in
244 glucose homeostasis. Note that the glucose turnover (i.e. % of the pool per min) was nearly identical
245 demonstrating that quantitation of tracer dilution was not affected by the intraperitoneal injection.

246

247 Figure 2 demonstrates the time-dependent measurements of glucose concentration and isotopic
248 enrichment in rodents following treatment with a PPAR- γ activator. Regardless of the model or the
249 specific compound, we observed a dramatic decrease in blood glucose (Panel A and C). Based on the
250 previous data that established a reasonable equivalence between the modalities for administering a
251 tracer (Figure 1 and Table 1), [U- 13 C]glucose was dosed here via an intraperitoneal injection. In the case
252 where we studied fZDF rats, we again observed a transient increase in plasma labeling as the tracer
253 slowly enters the systemic circulation (Panel B), this is not seen in ob/ob mice (Panel D) and reflects a
254 faster movement of tracer from the intraperitoneal space to the systemic circulating.

255
256 The effect of PPAR- γ treatment on the rate of endogenous glucose production was calculated from the
257 parameter estimates (i.e. pool size and fractional turnover rates) shown in Table 2. Treatment of fZDF
258 rats with Rosiglitazone substantially reduced endogenous glucose production (i.e. $\sim 18\%$, $p < 0.05$),
259 consistent with reports in the literature (22). As expected, Rosiglitazone led to a marked reduction in
260 fasting insulin concentration, which dramatically influenced the calculated “glucose production index”
261 (37). Similar observations were made in ob/ob mice following treatment with Pioglitazone. As expected,
262 Pioglitazone led to a dramatic decrease in blood glucose and endogenous glucose production (i.e. $\sim 28\%$,
263 $p < 0.01$) (22), note that in this case glucose production approached values that were observed in
264 control (ob+) mice ($p = 0.12$). Consistent with data that were obtained in the rat model, treatment of
265 ob/ob mice with Pioglitazone resulted in a marked reduction in the fasting insulin concentration, which
266 led a sizeable decrease in the “glucose production index”.

267
268 Another set of experiments was considered in both rodent models to cross-validate the data observed
269 to this point and to determine whether the calculated “glucose production index” would reflect clamp-
270 derived estimates of insulin sensitivity of endogenous glucose production, as suggested in humans (37).
271 Figure 3 demonstrates the primary data that were obtained when euglycemic-hyperinsulinemic clamps
272 were used to characterize the rats (Panel A - C) and mice (Panel D - F). An infusion of tracer amounts of
273 [U- 13 C]glucose was initiated during the basal period, to minimize a large shift in enrichment during the
274 clamp period a small amount of [U- 13 C]glucose was spiked into the exogenous glucose infusate. In all
275 cases we could clearly quantify the [13 C]labeling of glucose, Table 3 contains the glucose flux rate data
276 that are derived from the primary data contained in Figure 3. As expected, there was a marked
277 impairment in the ability of insulin to suppress endogenous glucose production in the vehicle-treated
278 disease models however both “glitazones” improved the insulin-mediated control of glucose production
279 in the respective models.

280
281 A final set of experiments was conducted to determine the potential of this approach in normal (control)
282 rats. For example, to this point most experiments had considered studies following the modulation of
283 glucose flux in a disease model, herein we asked whether the method could detect “normal” glucose
284 flux responses. Since it is known the glucose production will decrease with extended fasting (8), we
285 measured glucose production in short- vs long-term fasted states. Figure 5 demonstrates that extended
286 fasting leads to a somewhat lower basal glucose concentration, although the tracer administration
287 tended to increase the concentration of circulating glucose this was consistent across the groups. Based

288 on the enrichment that was achieved (~ 6%), and as expected based on the load of tracer that was given
289 (0.015 mg per kg), one expects that the transient rise in glucose (Figure 5, Panel A) is due to some degree
290 of stress that likely results from handling of the animals and not from a substrate-mediated
291 perturbation. As summarized in Table 4, it was possible to obtain estimates of glucose flux that compare
292 with values that one might expect, as well, we were able to observe a decrease in glucose production in
293 the overnight vs the 4 hour fasted states.

294

295 **Discussion**

296 Despite the wide-spread number of studies that are aimed at quantifying rates of endogenous glucose
297 production, there is a gap in the field when it comes to accessing a simple tracer method(s) for use in
298 rodent models in vivo. Unfortunately, the path to successful drug discovery and development is often
299 impeded by several challenges when implementing tracer methods. For example, while it is possible to
300 implant catheters in rodents (3; 32), it is often not practical to consider this in broader experimental
301 plans. This is especially true in cases where one aims to screen potential therapeutic compounds and/or
302 contrast various dosing schemes. Academic laboratories are faced with similar hurdles. For example,
303 although a given laboratory may aim to characterize a limited number of animal models and/or
304 conditions, the requisite expertise to implant catheters (or perform tail vein injections) may not exist.
305 Many academic centers, and indeed even the NIH, have sponsored core facilities to help support such
306 studies with better efficiency (2; 3; 21). Nevertheless, extra resources are required to transfer animals to
307 specialized laboratories.

308

309 Some investigators have appreciated the issues noted above and therein explored different modalities
310 for quantifying metabolic flux and phenotyping rodents. For example, Kurland and colleagues have
311 shown that one can deliver tracers using osmotic pumps (43). While we have found this logic to be
312 valuable in some instances (6), the use of mini-pumps imposes an extra cost and requires that animals
313 undergo a mild sedation (to place the device) which may affect acute readouts of glucose flux. Jones and
314 colleagues have been able to derive information regarding metabolic phenotypes using a variety of
315 novel approaches that also circumvent the use of catheters (11; 12; 23). In some cases certain novel
316 approaches can unmask phenotypes that are missed by “gold-standard” methods (36). If one considers
317 the seemingly unlimited number of models and/or therapeutic probes that can be generated, it is
318 expected that the development of simplified (but reliable) methods may yield new insight into factors
319 which regulate glucose homeostasis and affect the loss of glycemic control that is seen in Type 2
320 diabetes and insulin resistant states.

321

322 We hypothesized that one could quantify glucose flux by using an intraperitoneal injection to deliver a
323 glucose tracer. This is conceptually similar to the use of an intravenous bolus for administering a tracer
324 with two obvious caveats. First, one would need to obtain some knowledge regarding when to collect
325 samples. Ideally, one should wait until the tracer has completely entered (and mixed with) the plasma
326 compartment. Second, one would have to estimate a glucose pool size by assuming a volume of
327 distribution for glucose. For example, although it is possible to determine the pool size following an
328 intravenous bolus (i.e. pool size = mass injected tracer / initial labeling) (30; 41), this logic would not

329 hold in cases where the tracer slowly enters the circulation. We previously demonstrated that one could
330 obtain comparable rates of endogenous glucose production when using an infusion method vs a bolus
331 method in rats (25). Those studies assumed a volume of distribution that was equivalent to $\sim 20\%$ of
332 body mass. Provided that pool sizes do not dramatically change over the course of an experiment, it is
333 not surprising that one would obtain some agreement between the different approaches for
334 administering the glucose tracers (27; 28).

335
336 A particularly important caveat to consider is whether the amount of $[U-^{13}C_6]$ glucose would be
337 comparable to a true tracer load or whether it would perturb the metabolism under investigation. Based
338 on the rationale noted above one could derive an algorithm to examine the tracer load. For example,
339 the pool size can be estimated from the body weight and the basal glucose concentration, i.e. total mg
340 of glucose \sim body weight (g) \times 0.2 \times glucose concentration (mg per ml). For a 25 g mouse with “normal”
341 fasting glucose (i.e. ~ 1.25 mg per ml) one would expect a pool size of ~ 6.25 mg glucose. If we wanted to
342 reach a reasonable enrichment, e.g. $\sim 5\%$, we would multiply 6.25×0.05 and determine that the tracer
343 dose should be ~ 0.3 mg, or ~ 0.0125 mg per kg body weight. In cases where the basal glucose
344 concentration is higher than normal the tracer dose would simply be scaled accordingly (in proportion to
345 the change in glucose concentration) to ensure that one could reliably quantify the isotopic enrichment
346 and yet minimize the chance of altering the endogenous glucose concentration.

347
348 The studies outlined herein determined if we could reliably quantify rates of glucose production when a
349 tracer (e.g. $[U-^{13}C]$ glucose) is administered using an intraperitoneal bolus injection. Our initial set of
350 experiments aimed to directly contrast the use of an intravenous vs an intraperitoneal bolus of tracer.
351 Recognizing that investigators may use rats and mice interchangeably we thought to consider both
352 models. As expected, there is an exponential dilution of $[U-^{13}C]$ glucose following intravenous tracer
353 administration, note that the maximum enrichments were typically below 10% (when administering
354 0.05 g $[U-^{13}C]$ glucose per kg body weight in obese animals). Although those relatively low levels of
355 enrichment imply a minimum tracer-induced perturbation of metabolism it is obvious that the glucose
356 concentration was not always stable. For example, in the mouse model (Figure 1C) we detected an
357 increase in the concentration of circulating glucose immediately following the intravenous bolus. We
358 primarily attribute this to stress which likely results from the brief restraint that is required to perform
359 the tail vein injection. In our experience, some rat models are more stable to handling and manipulation
360 therefore these transient excursions in circulating glucose concentrations are typically not seen (Figure
361 1A).

362
363 As noted above, in cases where we administered the glucose tracer via an intraperitoneal injection we
364 assumed a volume of distribution that was equal to $\sim 20\%$ of the respective body weight. This yielded a
365 glucose pool size which was virtually identical to the pool size that was determined from the initial
366 dilution of $[U-^{13}C]$ glucose following the intravenous bolus in fZDF rats (Table 1). Glucose production
367 rates were then calculated by multiplying the respective pool sizes by the corresponding fractional
368 turnover rates (Table 1); those data suggested comparable estimates of flux regardless of the route by
369 which the tracer was administered. The absolute values that we obtained (i.e. ~ 6.75 mg \times kg $^{-1}$ \times min $^{-1}$)

370 are in reasonable agreement with the literature which suggested that the intravenous approach would
371 have merit in our rat model (7; 15; 29; 33-35).

372
373 Studies in a mouse model of insulin resistance and obesity led to similar overall conclusions regarding
374 the potential merit of using an intravenous bolus injection (Table 1) with one caveat. For example, we
375 observed comparable rates of tracer dilution (i.e. fractional turnover of the glucose pool) regardless of
376 the modality that was used to administer the tracer. The obvious caveat in the mouse model centers on
377 the sudden increase in glucose concentration following the intravenous injection (Figure 1C). As noted
378 earlier, if we had used the initial dilution method (i.e. pool size (mg) = tracer dose (mg) / initial labeling)
379 we would overestimate the glucose pool as compared to what we would infer by measuring the baseline
380 concentration and assuming a distribution volume that is ~ 20% of body weight (i.e. ~ 43 vs ~ 24 mg
381 shown Table 1). The ~ 1.8-fold difference in the apparent pool size is very consistent with the acute ~
382 1.6-fold change in glucose concentration that is seen within 5 minutes of giving an intravenous tracer
383 bolus, this most likely reflects some degree of stress that is associated with that modality.

384
385 When we estimated the volume of distribution, by assuming that it represents ~ 20% of body weight, we
386 calculated rates of glucose production that were similar (albeit statistically different) between mice
387 which were given an intravenous vs an intraperitoneal bolus of tracer (Table 1). Although the current
388 data set could not definitively explain the difference between the rates of glucose production between
389 the studies, we expect that the initial perturbation of glucose concentration following the intravenous
390 injection directly altered the metabolism under investigation. In our experience, the use of an
391 intraperitoneal injection typically leads to smoother profiles of circulating glucose concentration therein
392 providing the initial motivation for us to explore this route of tracer administration as a means of
393 facilitating studies. The absolute values of glucose production that we observed in the mouse study (i.e.
394 ~ 11 mg x kg⁻¹ x min⁻¹, Table 1) are comparable to reports in the literature (1; 2). Obviously there is a
395 caveat that the use of [U-¹³C]glucose would typically yield flux rates that are, if anything, lower than
396 reports that rely on [3-³H]glucose (3; 21) given the different metabolic fates of the respective labeled
397 glucose molecules (18-20).

398
399 Based on the agreement between the intravenous and intraperitoneal modes of tracer administration in
400 both rat and mouse studies, we were encouraged to examine the possibility of detecting changes in
401 glucose flux. It is well known that “glitazones” can modulate endogenous glucose production, although
402 the magnitude of those changes is not necessarily large the data are generally consistent across studies
403 (22). Therefore, rodents were either treated with Rosiglitazone or Pioglitazone for a given period and
404 glucose flux was examined following an intraperitoneal tracer administration (Figure 2). In cases where
405 we examined the fZDF rat model, we observed reasonable reductions in glucose production following
406 treatment with Rosiglitazone (Table 2). The magnitude of this effect was slightly greater in the
407 Pioglitazone-treated ob/ob mouse model, which approached values of glucose production that were
408 close to control animals (Table 2). From these studies we concluded that the use of an intraperitoneal
409 route of tracer administration should have some merit in helping investigators quantify rates of glucose
410 production in vivo. Specifically, we could observe different flux rates between lean and obese mice and

411 we could detect an improvement in the control of glucose homeostasis following drug treatment in rat
412 and mouse models (Table 2). Collectively, these data strongly suggest that the approach has merit.

413
414 Another set of experiments was initiated to contrast our intraperitoneal method for estimating glucose
415 production with data that would be obtained from comparable rodent models under euglycemic-
416 hyperinsulinemic clamp conditions. Specifically, attention was directed towards a comparison of the
417 logic that has been described by Vangipurapu et al (37). Briefly, although glucose-insulin clamps
418 represent a “gold-standard” for studying glucose homeostasis, it is obviously not practical to routinely
419 perform clamps especially as resources become limited. Since Vangipurapu et al have shown that it is
420 possible to derive an insulin sensitivity index of glucose production by simultaneously measuring glucose
421 production and prevailing insulin concentrations (37) we aimed to apply their logic in our preclinical
422 setting.

423
424 Our rodent models were subjected to glucose-insulin clamps in order to confirm the existence of
425 dysregulated glucose production in fZDF rats and ob/ob mice (Figure 3); those studies demonstrate a
426 substantially blunted suppression of glucose production in each model (Table 3). Since the data compare
427 very well with the calculated glucose production index for the respective models, our observations imply
428 that the “glucose production index” provides a useful surrogate of clamp-derived insulin sensitivity of
429 endogenous glucose production in rodent models (Figure 4). Clearly, the ability to derive this production
430 index (Table 2) is facilitated by the ability to easily determine rates of glucose production, which we
431 believe can be achieved via an intravenous route of tracer administration.

432
433 A final set of experiments aimed to quantify glucose flux under more normal conditions. For example,
434 the studies that have been considered to this point were primarily aimed at studying the fundamental
435 underlying concepts surrounding the tracer kinetics and to demonstrate the application in disease
436 models following drug treatment. As noted in Figure 2 and Table 2 this approach could quantify
437 differences in glucose flux between obese mice and lean controls, as well as determine the
438 pharmacological efficacy. Consistent with those observations, we were able to detect differences in
439 glucose production in short- vs long-term fasted rats (Figure 5 and Table 4). For example, it is generally
440 well known that extended fasting will result in lower glucose flux, i.e. hepatic glycogen stores become
441 depleted and glucose flux is dominated by the gluconeogenic contribution (8). Beylot and colleagues
442 clearly demonstrated the fasting will change total glucose flux (and the contribution of the respective
443 intra-hepatic flux rates) in rodents as seen in humans (24), our data (Figure 5 and Table 4) are in strong
444 agreement with the expected changes in glucose production. One point that is worth mentioning
445 centers on the absolute values of EGP reported here, which are somewhat lower than those reported in
446 other studies (17). A likely explanation has to do with the body mass, our rats were approximately twice
447 the size of those used in other studies. Since data are normalized to body weight this variable could
448 contribute to the lower rate of EGP.

449
450 To summarize our findings, we have considered the use of a novel modality for administering a glucose
451 tracer(s) which therein allows one to estimate rates of endogenous glucose production. We have

452 compared this approach, using direct experimentation, with previously accepted methods for
453 quantifying glucose kinetics in vivo. Our data demonstrate reasonable agreement between this new
454 approach and (i) the use of an intravenous route of tracer administration and (ii) the ability to detect
455 alterations in glucose production via glucose-insulin clamps. For example, we could couple these simple
456 estimates of basal glucose production and measurements of insulin levels and therein calculate a
457 glucose production index (37). Those values compare favorably with direct determinations of insulin-
458 mediated control of glucose production suggesting that one may be able to circumvent the use of
459 glucose-insulin clamps in some circumstances.

460
461 In conclusion, although intraperitoneal injections are typically used in studies of glucose tolerance and
462 as a route of drug delivery, it is also possible to administer glucose tracers using this route and therein
463 estimate endogenous flux rates. Presumably the approach that is outlined here will facilitate studies of
464 glucose production however one should still consider the fact that metabolic perturbations may occur in
465 some cases when a glucose tracer is administered using an intraperitoneal injection. The two other
466 important factors to consider are centered on assumptions regarding (i) when to collect samples and (ii)
467 how to estimate the volume of distribution. As noted, this can have an obvious impact on the absolute
468 rates of glucose production. In our experience it seems that rats and mice can be sampled ~ 45 and ~ 30
469 min after the tracer is injected, respectively. This delay between the tracer injection and initial sampling
470 should ensure that enrichment is being measured after the tracer has entered the systemic circulation.
471 Obviously, investigators can modify the sampling schedule as needed. Likewise, one would need to
472 consider whether any factor(s) might influence the entry of label into the plasma. For example, the
473 presence of ascites might slow the movement of tracer. As shown herein, even in cases where we have
474 studied obese (e.g. NAFLD/NASH-like) animals we were able to apply the logic and quantify glucose flux.
475

476 It is important to note that although the discussion to this point reflects in vivo data which support our
477 logic, we have also considered questions surrounding the timing of sample collection using a more
478 general modeling and simulation strategy (see Appendix). The exercise considered a case in which in the
479 analytical error is ~ 1% of the measured enrichment (this is in the range of the general assay conditions
480 that we have used). Namely, if we expect the initial enrichment to reach 5%, an analytical error of $\pm 1\%$
481 could lead to estimates of enrichment ranging from 4.95 to 5.05% (26). Since we have used [U-
482 $^{13}\text{C}_6$]glucose and there is no detectable natural background labeling, the overall method can tolerate
483 considerable analytical error (simulations demonstrated that reasonably good fits of the tracer dilution
484 could be obtained even if the analytical error approached 10%, not shown). We remind the reader that
485 mass spectrometry error in measuring enrichments is not the only factor to consider, for example, noise
486 in the glucose pool size (i.e. measurements of glucose concentration) would also contribute to variability
487 in the apparent glucose flux; therefore, attention to animal handling is also important. Presumably one
488 can most easily probe for differences between groups if body size and/or compositional changes are
489 minimal. Nevertheless, we were able to observe differences between ob/ob and ob/+ control mice. We
490 hope that the approach developed here can be of use to investigators who are focused on
491 understanding and manipulating glucose production.

492

494

495 **Figure legends**

496 **Figure 1. Characteristics of glucose concentration and isotopic enrichment in rodent models.** Post-
 497 absorptive blood samples were collected to determine the fasting glucose concentration. A tracer dose
 498 of [U-¹³C]glucose was administered using an intravenous (IV) or intraperitoneal (IP) bolus injection (t =
 499 0), samples were collected thereafter to measure the temporal profiles of glucose concentration and
 500 enrichment. Panel A and B contain profiles that were obtained in fZDF rats whereas Panel C and D
 501 contain data that were obtained in high-fat fed C57Bl/6J mice. Data are shown as mean ± sem.

502

503 **Figure 2. Glitazone-mediated modulation of glucose homeostasis in rodents.** Rosiglitazone or vehicle
 504 (methylcellulose) was mixed with the diet and fed for 5 days to the respective groups of fZDF rats, ob/ob
 505 mice were treated with Pioglitazone under a comparable paradigm. Post-absorptive blood samples were
 506 then collected to determine the fasting glucose concentration. A tracer dose of [U-¹³C]glucose was
 507 administered using an intraperitoneal (IP) bolus injection (t = 0), samples were collected thereafter to
 508 measure the temporal profiles of glucose concentration and enrichment. Panel A and B contain data
 509 from fZDF rats whereas Panel C and D contain data from ob/ob mice. Data are shown as mean ± sem.

510

511 **Figure 3. Glucose-insulin clamps in rodents.** Rosiglitazone (5 mg per kg) or vehicle (methyl-cellulose)
 512 was orally dosed in fZDF rats for 5 days and ob/ob mice were treated with Pioglitazone (30 mg per kg)
 513 mixed in the diet for 4 weeks. Post-absorptive blood samples were then collected to determine the
 514 fasting glucose concentration. An infusion of [U-¹³C₆]glucose was used to estimate glucose flux during a
 515 baseline period (sampled at t = -10 and 0 minutes) and during a hyperinsulinemic-euglycemic clamp
 516 period (starting at t = 0 minutes and sampled for enrichment measurements over the last 40 min of the
 517 study). Data are shown as the mean ± sem for rats (Panels A-C) and mice (Panels D-F). Data are shown as
 518 mean ± sem.

519

520 **Figure 4. Measuring insulin sensitivity of endogenous glucose production: Comparison of a glucose-**
 521 **insulin clamp vs a glucose production index.** Data from the respective studies discussed herein were
 522 compared against each other. As explained in the Materials and Methods, the glucose production index
 523 reflects the product of endogenous glucose production (EGP) and circulating insulin concentration. The
 524 % suppression of EGP reflects the change in EGP from baseline vs the steady-state period of the clamp.
 525 Comparisons are shown using mean ± sem, square and circles represent data in ob/ob mice and fZDF
 526 rats, respectively, solid and open symbols represent baseline untreated disease models and “glitazone”
 527 treated, respectively.

528

529 **Figure 5. Effect of nutritional status on glucose flux in vivo.** Sprague-Dawley rats were given on
 530 intraperitoneal tracer dose of [U-¹³C]glucose, samples were collected thereafter to measure the
 531 temporal profiles of glucose concentration (Panel A) and enrichment (Panel B). The overall glucose
 532 concentration profile was lower with longer fasting, enrichment profiles matched the general trend that
 533 is seen in other studies, i.e. there is a delay phase of entry over the initial ~ 30 min followed by a dilution
 534 of the labeling to the end of the study. Data are shown as mean ± sem (n = 8 per group).

535

536 **List of Tables.**

537 Table 1. Glucose production in rodent models. Kinetic parameters including glucose turnover and pool
 538 size were estimated from the primary data (Figure 1). Rates of endogenous glucose production (EGP)
 539 were calculated as described in Materials and Methods. Statistical analyses were performed using 2-
 540 tailed t-tests and assuming equal variance, no differences were observed in any measurements for fZDR
 541 rats, * represents p = 0.02 for EGP in high-fat (HF) fed mice.

542

	fZDF rats (n = 6-7 per group)		HF-fed C57BL/6J mice (n = 7-8 per group)	
	IV bolus	IP bolus	IV bolus	IP bolus
Body weight (g)	289 ± 5	286 ± 4	54.2 ± 1.1	53.7 ± 0.6
Turnover (% pool per min,45→120 min)	1.83 ± 0.29	1.86 ± 0.25	2.70 ± 0.16	2.36 ± 0.10
Pool size (mg)	112 ± 11	111 ± 15	24.5 ± 1.2	24.1 ± 1.0
EGP (mg/kg/min)	6.91 ± 0.81	6.55 ± 0.58	11.9 ± 0.5	10.5 ± 0.3*

543

544

545 Table 2. Glucose production in rodents following treatment with either Rosiglitazone or Pioglitazone. Kinetic parameters including glucose
 546 turnover and pool size were estimated from the primary data (Figure 2), rates of endogenous glucose production (EGP) were calculated as
 547 described in Materials and Methods. The glucose production index was calculated as described (37). For studies in fZDF rats, statistical analyses
 548 were performed using 2-tailed t-tests and assuming equal variance where * represents $p < 0.05$. For studies done in obese mice, statistical
 549 analyses were done using ANOVA with Tukey's post-hoc testing across all groups where * represents $p < 0.05$ between Vehicle and Pioglitazone
 550 of ob/+ vehicle and # $p < 0.05$ between Pioglitazone and ob/+ vehicle.
 551

	fZDF rats (n = 6-9 per group)		ob/ob mice (n = 7-8 per group)		
	Vehicle	Rosiglitazone	Vehicle	Pioglitazone	ob/+, vehicle
Body weight (g)	302 ± 3	342 ± 6*	45.9 ± 0.9	46.2 ± 0.7	26.3 ± 0.4*
Turnover (% pool per min, 45→120 min)	1.67 ± 0.19	3.43 ± 0.25*	1.93 ± 0.09	2.39 ± 0.19*	2.17 ± 0.05
Pool size (mg)	165 ± 24	77 ± 7*	27.6 ± 1.4	16.3 ± 0.7*	9.2 ± 0.3*#
EGP (mg/kg/min)	9.33 ± 0.56	7.58 ± 0.54*	11.8 ± 0.9	8.4 ± 0.5*	7.5 ± 0.2*
Insulin (ng/ml)	5.81 ± 0.45	1.04 ± 0.12*	27.9 ± 2.3	5.4 ± 1.4*	0.1 ± 0.02*#
Glucose production index (EGP x [insulin])	54.6 ± 9.5	7.0 ± 0.6*	316 ± 27	46 ± 12*	0.92 ± 0.02*#

552
 553 Table 3. Glucose kinetics as determined using a tracer infusion protocol coupled with a euglycemic-hyperinsulinemic clamp. Glucose flux rates,
 554 including the rate of appearance (Ra) and endogenous glucose production (EGP) were determined in different rodent models following
 555 treatment with the respective PPAR- γ activators or methyl-cellulose vehicle. Statistical analyses were performed using 2-tailed t-tests and
 556 assuming equal variance, * represents $p = 0.05$.
 557

	fZDF rats (n = 6-8 per group)		ob/ob mice (n = 6-8 per group)	
	Vehicle	Rosiglitazone	Vehicle	Pioglitazone
Body weight (g)	322 ± 6	349 ± 8*	47.5 ± 0.4	50.1 ± 1.3
Basal Ra (mg/kg/min)	8.3 ± 0.5	7.8 ± 0.4	43.5 ± 9.3	32.8 ± 5.1
Clamp Ra (mg/kg/min)	10.9 ± 3.2	29.8 ± 2.5*	29.3 ± 4.1	43.4 ± 3.1*
Clamp EGP (mg/kg/min)	5.1 ± 1.2	2.8 ± 0.6*	24.3 ± 5.1	2.4 ± 1.2*
% suppression of EGP	38 ± 13	69 ± 7#	37 ± 7	95 ± 4*

558

559 Table 4. Effect of nutritional status on glucose production. Kinetic parameters including glucose turnover and pool size were estimated from the
 560 primary data (Figure 5). Rates of endogenous glucose production (EGP) were calculated as described in Materials and Methods. Statistical
 561 analyses were performed using a paired t-test, * represents $p < 0.01$ and ** $p = 0.05$.
 562

	Sprague-Dawley rats (n = 8 per study)	
	4 hour fast	overnight fast
Body weight (g)	535 ± 3	519 ± 3*
Turnover (% pool per min, 45→150 min)	1.74 ± 0.21	1.39 ± 0.11**
Pool size (mg)	117 ± 5	95 ± 3*
EGP (mg/kg/min)	3.8 ± 0.5	2.6 ± 0.2*

563

564
565
566
567
568

Reference List

- 569 1. **Ayala JE, Bracy DP, Malabanan C, James FD, Ansari T, Fueger PT, McGuinness OP and**
570 **Wasserman DH.** Hyperinsulinemic-euglycemic clamps in conscious, unrestrained mice. *J Vis Exp*
571 2011.
- 572 2. **Ayala JE, Bracy DP, McGuinness OP and Wasserman DH.** Considerations in the design of
573 hyperinsulinemic-euglycemic clamps in the conscious mouse. *Diabetes* 55: 390-397, 2006.
- 574 3. **Ayala JE, Samuel VT, Morton GJ, Obici S, Croniger CM, Shulman GI, Wasserman DH and**
575 **McGuinness OP.** Standard operating procedures for describing and performing metabolic tests
576 of glucose homeostasis in mice. *Dis Model Mech* 3: 525-534, 2010.
- 577 4. **Baker N and HUEBOTTER R.** GLUCOSE METABOLISM IN MICE. *Am J Physiol* 207: 1155-1160,
578 1964.
- 579 5. **Baker N, Shipley RA, Clark RE and INCEFY GE.** C14 studies in carbohydrate metabolism: glucose
580 pool size and rate of turnover in the normal rat. *Am J Physiol* 196: 245-252, 1959.
- 581 6. **Bederman IR, Foy S, Chandramouli V, Alexander JC and Previs SF.** Triglyceride Synthesis in
582 Epididymal Adipose Tissue CONTRIBUTION OF GLUCOSE AND NON-GLUCOSE CARBON SOURCES.
583 *Journal of Biological Chemistry* 284: 6101-6108, 2009.
- 584 7. **Bergeron R, Yao J, Woods JW, Zychband EI, Liu C, Li Z, Adams A, Berger JP, Zhang BB, Moller DE**
585 **and Doebber TW.** Peroxisome proliferator-activated receptor (PPAR)-alpha agonism prevents
586 the onset of type 2 diabetes in Zucker diabetic fatty rats: A comparison with PPAR gamma
587 agonism. *Endocrinology* 147: 4252-4262, 2006.
- 588 8. **Chandramouli V, Ekberg K, Schumann WC, Kalhan SC, Wahren J and Landau BR.** Quantifying
589 gluconeogenesis during fasting. *Am J Physiol* 273: E1209-E1215, 1997.
- 590 9. **DeFronzo RA and Ferrannini E.** Regulation of hepatic glucose metabolism in humans. *Diabetes*
591 *Metab Rev* 3: 415-459, 1987.
- 592 10. **DeFronzo RA, Ferrannini E and Simonson DC.** Fasting hyperglycemia in non-insulin-dependent
593 diabetes mellitus: contributions of excessive hepatic glucose production and impaired tissue
594 glucose uptake. *Metabolism* 38: 387-395, 1989.
- 595 11. **Delgado TC, Barosa C, Nunes PM, Cerdan S, Geraldes CF and Jones JG.** Resolving the sources of
596 plasma glucose excursions following a glucose tolerance test in the rat with deuterated water
597 and [U-13C]glucose. *PLoS One* 7: e34042, 2012.
- 598 12. **Delgado TC, Pinheiro D, Caldeira M, Castro MM, Geraldes CF, Lopez-Larrubia P, Cerdan S and**
599 **Jones JG.** Sources of hepatic triglyceride accumulation during high-fat feeding in the healthy rat.
600 *NMR Biomed* 22: 310-317, 2009.
- 601 13. **Erion DM, Lapworth A, Amor PA, Bai G, Vera NB, Clark RW, Yan Q, Zhu Y, Ross TT, Purkal J,**
602 **Gorgoglione M, Zhang G, Bonato V, Baker L, Barucci N, D'Aquila T, Robertson A, Aiello RJ, Yan**
603 **J, Trimmer J, Rolph TP and Pfeifferkorn JA.** The hepatoselective glucokinase activator PF-
604 04991532 ameliorates hyperglycemia without causing hepatic steatosis in diabetic rats. *PLoS*
605 *One* 9: e97139, 2014.

- 606 14. **Ferrannini E, Smith JD, Cobelli C, Toffolo G, Pilo A and DeFronzo RA.** Effect of insulin on the
607 distribution and disposition of glucose in man. *J Clin Invest* 76: 357-364, 1985.
- 608 15. **Fujimoto Y, Torres TP, Donahue EP and Shiota M.** Glucose toxicity is responsible for the
609 development of impaired regulation of endogenous glucose production and hepatic glucokinase
610 in Zucker diabetic fatty rats. *Diabetes* 55: 2479-2490, 2006.
- 611 16. **Gastaldelli A, Coggan AR and Wolfe RR.** Assessment of methods for improving tracer estimation
612 of non-steady-state rate of appearance. *J Appl Physiol (1985)* 87: 1813-1822, 1999.
- 613 17. **Jin ES, Jones JG, Burgess SC, Merritt ME, Sherry AD and Malloy CR.** Comparison of [3,4-
614 ¹³C₂]glucose to [6,6-²H₂]glucose as a tracer for glucose turnover by nuclear magnetic
615 resonance. *Magn Reson Med* 53: 1479-1483, 2005.
- 616 18. **Katz J and Dunn A.** Glucose-2-t as a tracer for glucose metabolism. *Biochemistry* 6: 1-5, 1967.
- 617 19. **Katz J, Dunn A, Chenoweth M and Golden S.** Determination of synthesis, recycling and body
618 mass of glucose in rats and rabbits in vivo ³H-and ¹⁴C-labelled glucose. *Biochem J* 142: 171-183,
619 1974.
- 620 20. **Katz J, Golden S, Dunn A and Chenoweth M.** Estimation of glucose turnover in rats in vivo with
621 tritium labeled glucoses. *Hoppe Seylers Z Physiol Chem* 357: 1387-1394, 1976.
- 622 21. **McGuinness OP, Ayala JE, Laughlin MR and Wasserman DH.** NIH experiment in centralized
623 mouse phenotyping: the Vanderbilt experience and recommendations for evaluating glucose
624 homeostasis in the mouse. *Am J Physiol Endocrinol Metab* 297: E849-E855, 2009.
- 625 22. **Natali A and Ferrannini E.** Effects of metformin and thiazolidinediones on suppression of
626 hepatic glucose production and stimulation of glucose uptake in type 2 diabetes: a systematic
627 review. *Diabetologia* 49: 434-441, 2006.
- 628 23. **Nunes PM, Jarak I, Heerschap A and Jones JG.** Resolving futile glucose cycling and
629 glycogenolytic contributions to plasma glucose levels following a glucose load. *Magn Reson Med*
630 71: 1368-1373, 2014.
- 631 24. **Peroni O, Large V and Beylot M.** Measuring gluconeogenesis with [2-¹³C]glycerol and mass
632 isotopomer distribution analysis of glucose. *Am J Physiol* 269: E516-E523, 1995.
- 633 25. **Previs S, Ciraolo ST, Agarwal KC, Soloviev MV and Brunengraber H.** Use of [6(H-2)-H-2]Glucose
634 and of Low Enrichment [U-(C-6)-C-13]Glucose for Sequential Measurements of Glucose-
635 Turnover. *Faseb Journal* 7: A288, 1993.
- 636 26. **Previs SF, Herath K, Castro-Perez J, Mahsut A, Zhou H, McLaren DG, Shah V, Rohm RJ, Stout SJ,
637 Zhong W, Wang SP, Johns DG, Hubbard BK, Cleary MA and Roddy TP.** Effect of Error
638 Propagation in Stable Isotope Tracer Studies: An Approach for Estimating Impact on Apparent
639 Biochemical Flux. *Methods Enzymol* 561: 331-358, 2015.
- 640 27. **Radziuk J and Pye S.** Quantitation of basal endogenous glucose production in Type II diabetes:
641 importance of the volume of distribution. *Diabetologia* 45: 1053-1084, 2002.
- 642 28. **Radziuk J and Pye S.** Tracer-determined glucose fluxes in health and type 2 diabetes: basal
643 conditions. *Best Pract Res Clin Endocrinol Metab* 17: 323-342, 2003.
- 644 29. **Satapati S, He T, Inagaki T, Potthoff M, Merritt ME, Esser V, Mangelsdorf DJ, Kliewer SA,
645 Browning JD and Burgess SC.** Partial resistance to peroxisome proliferator-activated receptor-
646 alpha agonists in ZDF rats is associated with defective hepatic mitochondrial metabolism.
647 *Diabetes* 57: 2012-2021, 2008.
- 648 30. **Shiple RA and Clark RE.** *Tracer methods for in vivo kinetics. Theory and applications.* New York:
649 Academic Press, 1972.
- 650 31. **Shulman GI, Ladenson PW, Wolfe MH, Ridgway EC and Wolfe RR.** Substrate cycling between
651 gluconeogenesis and glycolysis in euthyroid, hypothyroid, and hyperthyroid man. *J Clin Invest*
652 76: 757-764, 1985.

- 653 32. **Smith D, Rossetti L, Ferrannini E, Johnson CM, Cobelli C, Toffolo G, Katz LD and DeFronzo RA.**
654 In vivo glucose metabolism in the awake rat: tracer and insulin clamp studies. *Metabolism* 36:
655 1167-1174, 1987.
- 656 33. **Torres TP, Catlin RL, Chan R, Fujimoto Y, Sasaki N, Printz RL, Newgard CB and Shiota M.**
657 Restoration of hepatic glucokinase expression corrects hepatic glucose flux and normalizes
658 plasma glucose in Zucker diabetic fatty rats. *Diabetes* 58: 78-86, 2009.
- 659 34. **Torres TP, Fujimoto Y, Donahue EP, Printz RL, Houseknecht KL, Treadway JL and Shiota M.**
660 Defective glycogenesis contributes toward the inability to suppress hepatic glucose production
661 in response to hyperglycemia and hyperinsulinemia in Zucker diabetic fatty rats. *Diabetes* 60:
662 2225-2233, 2011.
- 663 35. **Ueta K, O'Brien TP, McCoy GA, Kim K, Healey EC, Farmer TD, Donahue EP, Condren AB, Printz
664 RL and Shiota M.** Glucotoxicity targets hepatic glucokinase in Zucker diabetic fatty rats, a model
665 of type 2 diabetes associated with obesity. *Am J Physiol Endocrinol Metab* 306: E1225-E1238,
666 2014.
- 667 36. **Vaitheesvaran B, Chueh FY, Xu J, Trujillo C, Saad MF, Lee WN, McGuinness OP and Kurland IJ.**
668 Advantages of dynamic "closed loop" stable isotope flux phenotyping over static "open loop"
669 clamps in detecting silent genetic and dietary phenotypes. *Metabolomics* 6: 180-190, 2010.
- 670 37. **Vangipurapu J, Stancakova A, Kuulasmaa T, Paananen J, Kuusisto J, Ferrannini E and Laakso M.**
671 A novel surrogate index for hepatic insulin resistance. *Diabetologia* 54: 540-543, 2011.
- 672 38. **Vella A and Rizza RA.** Application of isotopic techniques using constant specific activity or
673 enrichment to the study of carbohydrate metabolism. *Diabetes* 58: 2168-2174, 2009.
- 674 39. **Wan M, Leavens KF, Hunter RW, Koren S, Wilamowitz-Moellendorff A, Lu M, Satapati S, Chu
675 Q, Sakamoto K, Burgess SC and Birnbaum MJ.** A noncanonical, GSK3-independent pathway
676 controls postprandial hepatic glycogen deposition. *Cell Metab* 18: 99-105, 2013.
- 677 40. **Weiss M.** Modelling of initial distribution of drugs following intravenous bolus injection. *Eur J
678 Clin Pharmacol* 24: 121-126, 1983.
- 679 41. **Wolfe RR and Chinkes DL.** *Isotope tracers in metabolic research: Principles and practice of
680 kinetic analyses.* Hoboken, NJ: Wiley-Liss, 2005.
- 681 42. **Wong KP, Sha W, Zhang X and Huang SC.** Effects of administration route, dietary condition, and
682 blood glucose level on kinetics and uptake of ¹⁸F-FDG in mice. *J Nucl Med* 52: 800-807, 2011.
- 683 43. **Xu J, Xiao G, Trujillo C, Chang V, Blanco L, Joseph SB, Bassilian S, Saad MF, Tontonoz P, Lee WN
684 and Kurland IJ.** Peroxisome proliferator-activated receptor alpha (PPARalpha) influences
685 substrate utilization for hepatic glucose production. *J Biol Chem* 277: 50237-50244, 2002.
686
687
688
689
690
691
692
693
694
695
696

697 **Appendix. Application of modeling and simulation to validate the logic and optimize protocol designs.**

698 We used a modeling and simulation approach to assess the propagation of error in this overall method,
 699 and to understand how the sampling parameters and data analysis methods could impact studies.
 700 Figure 1 demonstrates that the absorption and distribution of the intraperitoneal [U-¹³C]glucose can be
 701 modeled using a two-compartment model.

702

703 The analytical solutions to the differential equations describing this system are given by:

704

$$[G_c^{lbl}(t)] = \frac{a}{a-k} (e^{-k \cdot t} - e^{-a \cdot t}) \frac{F \cdot G_d^{lbl}(t=0)}{V_c}$$

705

706

$$EGP(t) = V_c \left\{ \frac{d}{dt} [G_c(t)] + k \cdot [G_c(t)] \right\}$$

707

708 where “a” and “k” are rate constants, “F” is the bioavailability, and “G^{lbl}” and “G” represent the
 709 concentrations of ¹³C-labeled and endogenous (naturally labeled) glucose, respectively. Here we see that
 710 the key parameter for the calculation of EGP is the decay constant “k”, as the concentrations of the
 711 labeled and unlabeled glucose pools are, in principle, measurable through traditional analytical
 712 techniques. This decay constant can be determined by fitting the data with a double or single
 713 exponential function, depending on whether the plasma glucose data is taken early (where the
 714 absorption coefficient “a” dominates) or late (where the decay constant “k” dominates).

715

716 Using this model, we performed simulations to examine how error propagation through this system
 717 would impact the outcomes. We considered the use of two fitting methods to determine the optimal
 718 sampling protocol, i.e. that which yields a value of “k” closest to the theoretical value and with the least
 719 variance. The following parameters were used in the model: “a” = 0.1 min⁻¹, “F” = 95%, “V_d” = 200 ml per
 720 kg, tracer dose = 50 mg per kg. The errors in the total and ¹³C-glucose measurements were modeled
 721 using values for precision that are found in typical studies and based on our previous experience.
 722 Furthermore we assumed animal handling considerations would allow a maximum of ~ 7 plasma
 723 samples at a minimum interval of 15 minutes. Using these model assumptions, values for the theoretical
 724 time course of plasma ¹³C-glucose were calculated for three values of “k” (i.e. 0.015, 0.030 and 0.045 per
 725 min) which span a reasonably expected physiological range. A Monte Carlo approach was then used to
 726 add error to each ¹³C-glucose value and “k” was estimated using both a single and double exponential
 727 fit. This process was repeated 10,000 times and the resulting distribution of “k” values was used to
 728 calculate the mean value along with 95% confidence intervals for “k” (Figure 2).

729

730 The overall feasibility of using the intraperitoneal route to deliver a glucose tracer is reasonable. For
 731 example, Figure 2 demonstrates that the single and double exponential fits each yield reliable estimates
 732 of glucose turnover. As expected, the results suggest that for early sampling times, the single
 733 exponential fit will underestimate the correct value for “k”. The double exponential fit, while producing
 734 more accurate estimates for “k”, results in larger variance. From these simulations we concluded that a
 735 reasonable protocol (i.e. that which will most likely yield an accurate value for “k” with least variance) is

736 to sample ~ 45 to 150 minute after administering the glucose tracer and to use a single decaying
737 exponential fit to estimate “k”. Obviously, a strict adherence to these conditions is not essential, it is
738 expected that investigators will likely need to adjust the protocol as needed since there may be other
739 constraints that affect the design. The model and simulations outlined here give some general guidance
740 regarding the applicability of this method.
741

742 **Appendix Figure Legends.**

743 **Figure 1. Mathematical model of glucose metabolism following an intraperitoneal bolus**
744 **administration.** Different compartments are used to describe the absorption and metabolism.

745

746 **Figure 2. Effect of error on estimates of glucose turnover.** The fractional turnover of glucose was
747 assumed to range from 0.015 to 0.045 pools per min. It was expected that a tracer would be injected
748 using an intraperitoneal bolus at $t = 0$ minutes and that enrichment could be measured using samples
749 that were collected for up to 180 minutes. Panels A vs B reflect the apparent fractional turnover (mean \pm
750 standard deviation) if we used a single vs double exponential fit, respectively.

751

752

753

754

755

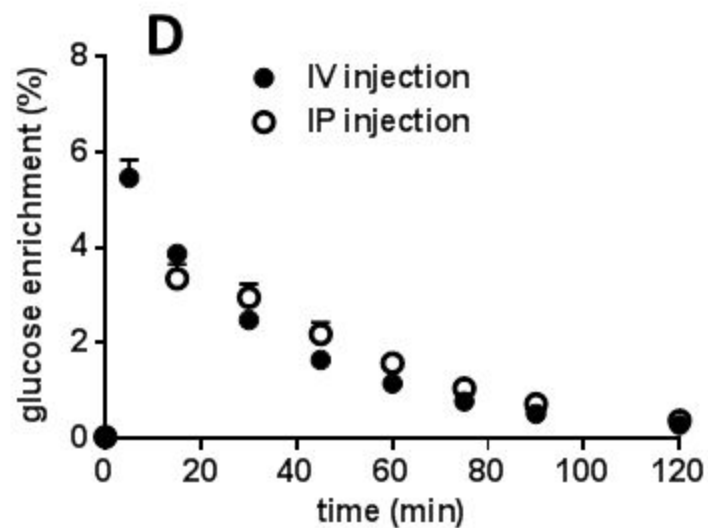
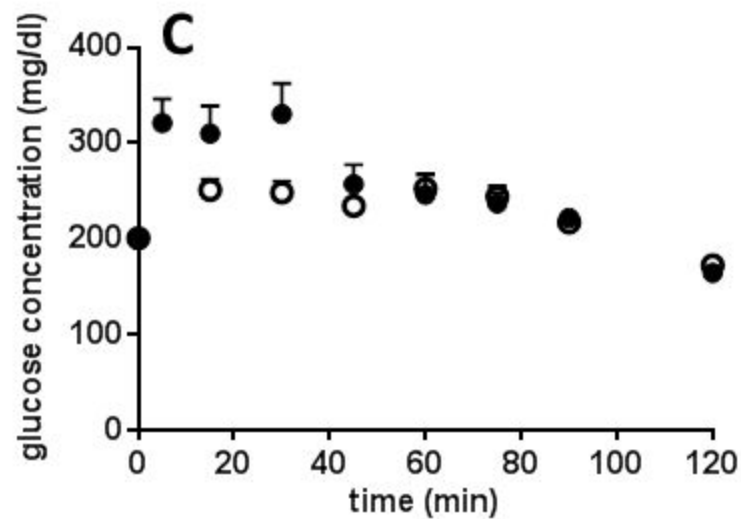
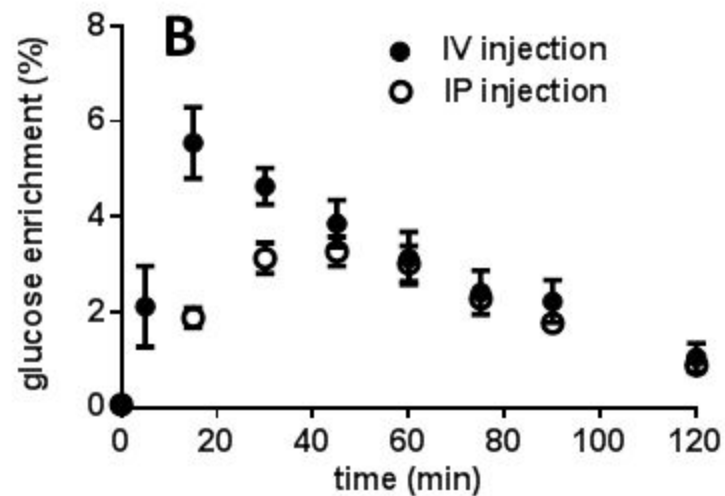
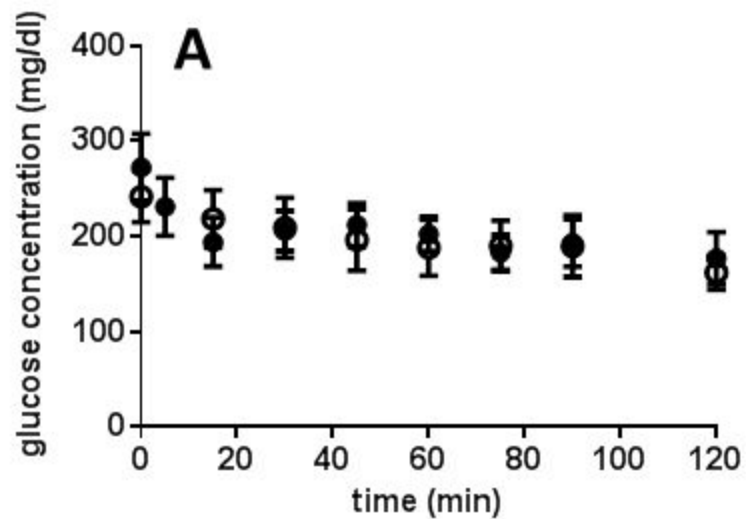


Figure 1

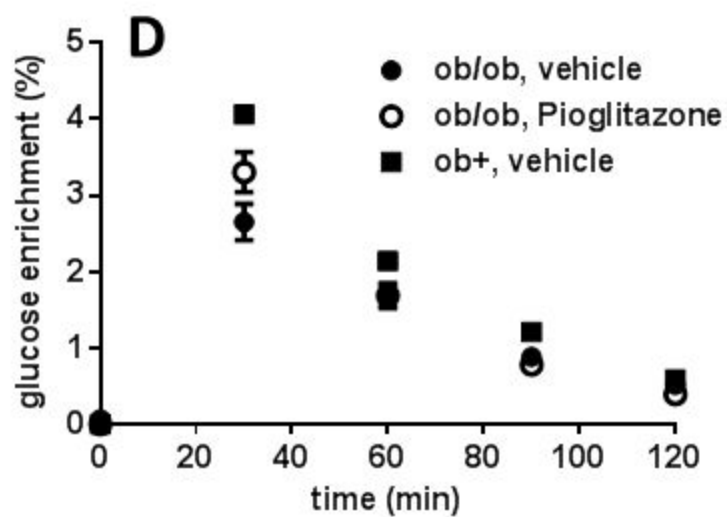
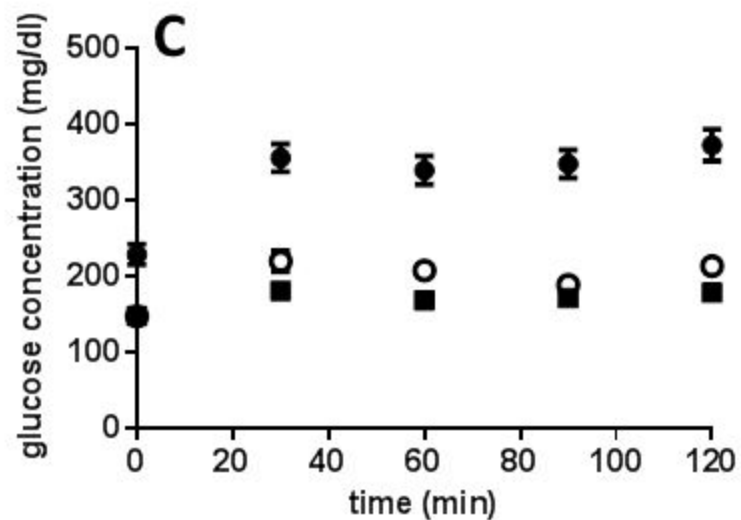
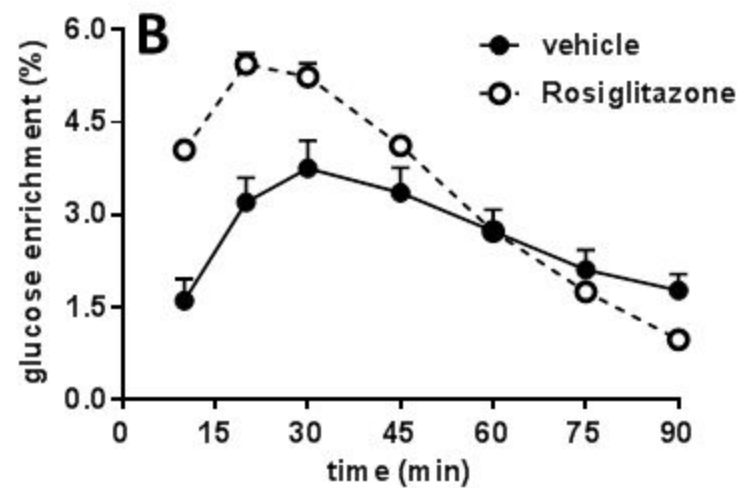
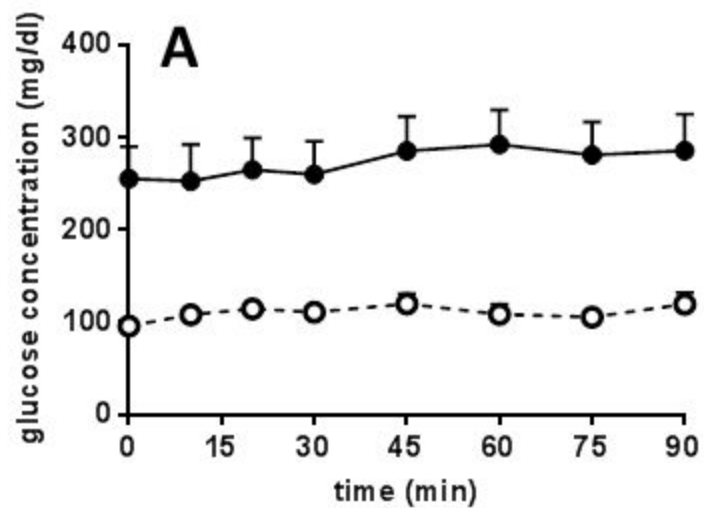


Figure 2

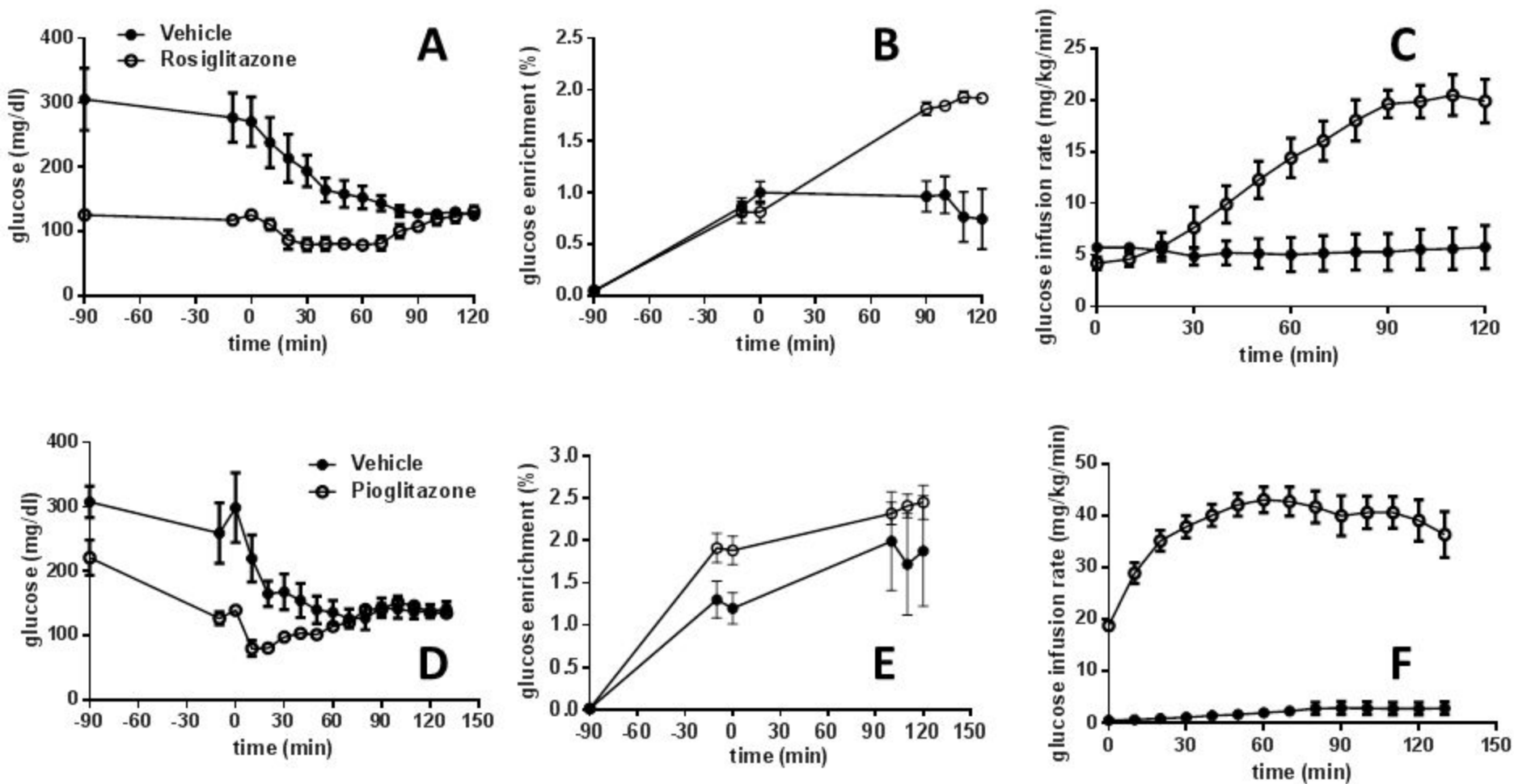


Figure 3

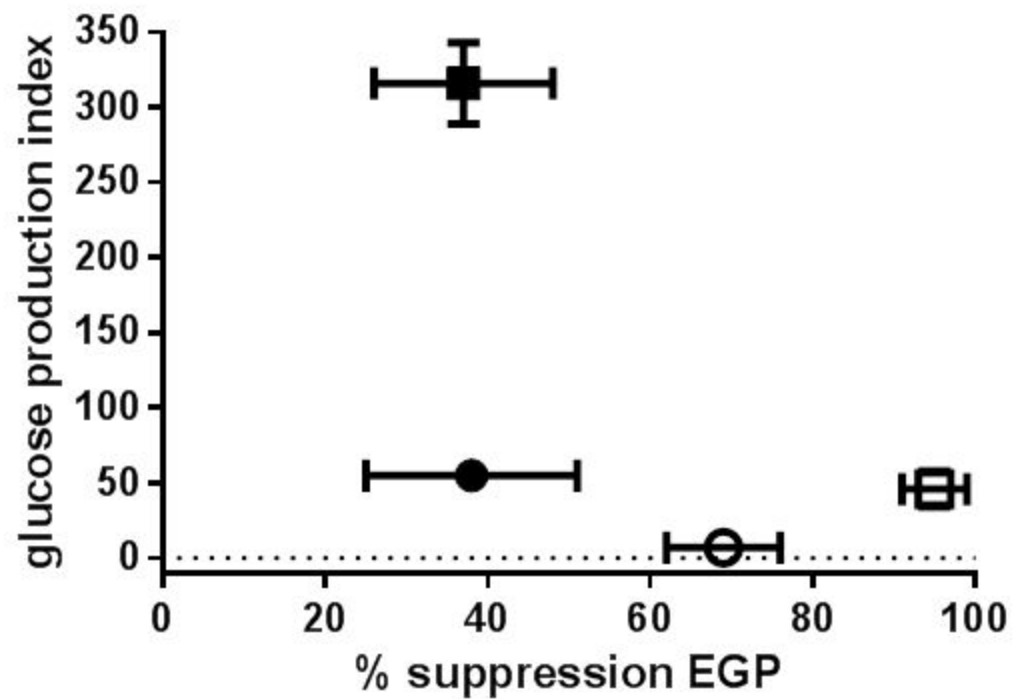


Figure 4

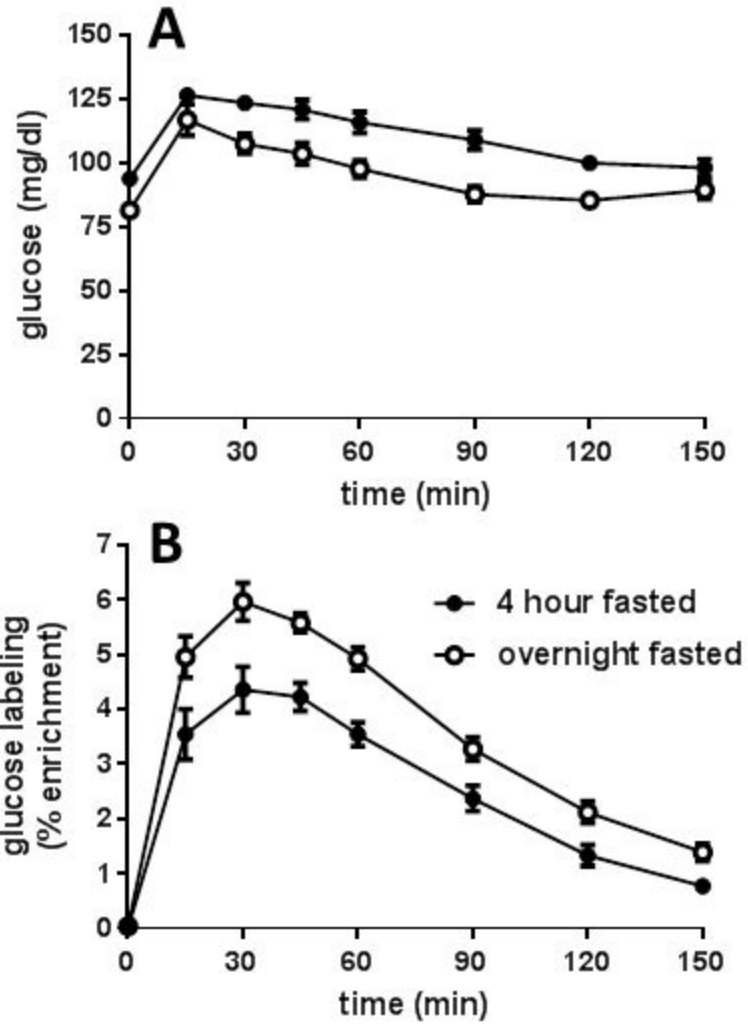


Figure 5

